

Classifying Superradiance in Extended Media

Paolo Longo,* Christoph H. Keitel, and Jörg Evers

Max Planck Institute for Nuclear Physics, Saupfercheckweg 1, 69117 Heidelberg, Germany

(Dated: June 4, 2022)

Single-photon superradiance is studied in a homogeneous, extended sample of two-level atoms in $d = 1, 2, 3$ dimensions. Based on a general functional form for the inter-atomic couplings, our description covers a wide range of possible electromagnetic reservoirs. We derive a criterion for the emergence of superradiant states as a function of the dimension and the type of the atom–atom coupling. We then exploit the scaling properties of the decay rate’s enhancement factor to categorize and compare superradiant states across different physical realizations, providing a bridge between the various theoretical and experimental approaches to superradiance in extended media.

PACS numbers: 42.50.Nn, 42.50.Ct

The coupling of single photons to ensembles of atoms is at the heart of light-matter interaction and quantum optics. Due to the coupling to an environment, a single atom is usually subject to spontaneous emission and experiences a frequency shift referred to as the Lamb shift. However, in an aggregation of atoms coupled via the radiation field, collective effects can significantly alter the properties compared to a single emitter. For instance, this was realized by Dicke [1, 2], who showed that N identical atoms which are confined to a volume much smaller than a wavelength cubed (the so-called small-volume limit) collectively behave as one “super atom”. This leads to exaggerated properties such as an acceleration of spontaneous decay by a factor of $\chi_{\text{Dicke}} = N$ (known as superradiance or an enhanced frequency shift (sometimes also termed “collective Lamb shift”).

Recently, the coherent emission from *extended* ensembles of emitters, has become the focus of experimental and theoretical investigations. The systems considered cover a wide range of possible realizations, including atoms near a nanofiber [3], thin vapor layers [4], cold ensembles of Rb atoms [5], or thin-film cavities with embedded Mössbauer nuclei in the realm of x-ray quantum optics [6–11]. Especially in the latter example, superradiance is realized even though minimal interatomic distance a exceeds the wavelength λ_0 .

Theoretical studies beyond Dicke’s small-volume limit focus on the modification of key quantities such as the collective decay rate (or frequency shift) due to special geometric arrangements of atoms, e.g., spherical clouds [12–15] or slabs [12, 16]. For these situations, the temporal dynamics and the emission spectrum have been discussed [12, 15]. In this context, it is usually assumed that the atoms are embedded in three-dimensional free space. However, this is not always the case as the recent experiments [6–10] employ a nuclear ensemble which is effectively embedded in just two spatial dimensions.

This generally raises the question if and how superradiance can be classified and compared across different

atomic systems. For instance, how does the existence of superradiant states depend on the ensemble dimensionality and the inter-atomic coupling? How do experimentally relevant quantities such as the particle number N , the sample volume \mathcal{V} , or the number density $\rho = N/\mathcal{V}$ influence decay rates (and frequency shifts)? Can superradiant states from different physical systems (e.g., with different dimensionality) be related to each other?

Here, we answer these questions in the context of a homogeneous, extended sample of two-level atoms in $d = 1, 2, 3$ dimensions. In particular, we provide a condition for the emergence of superradiant states as a function of the dimension and the type of the inter-atomic coupling. We then analyze the decay rates and frequency shifts across the different realizations in detail. This allows us to categorize and compare superradiant states in different physical systems by utilizing the scaling properties of the decay rate’s enhancement factor. Our findings, supported by examples of practical relevance, ultimately lead to a more general view on—and thus a deeper understanding of—superradiance in extended media.

Formulation of the Problem.— We start with a single two-level atom, representing the basic building block of our model (bare transition frequency $\omega_0 = ck_0$, $k_0 = 2\pi/\lambda_0$, and c the speed of light). The atom is embedded in an electromagnetic environment, e.g., free space, and is characterized by its spontaneous decay rate $\text{Re}(V_0) \equiv \gamma_0$ (we assume Markovian reservoirs [17]). The coupling to the environment also results in a frequency shift $\text{Im}(V_0)/2 \equiv \delta\omega_0$ (single-atom Lamb shift). In the presence of an identical, second atom, photons can be exchanged between the two atoms. Due to irreversible loss to the reservoir, the coupling $V_{\mathbf{r}_i\mathbf{r}_j} = \gamma_{\mathbf{r}_i\mathbf{r}_j} + 2i\delta\omega_{\mathbf{r}_i\mathbf{r}_j}$ is complex [17–21]. Here, $\gamma_{\mathbf{r}_i\mathbf{r}_j}$ ($\delta\omega_{\mathbf{r}_i\mathbf{r}_j}$) represents the real-valued cross-damping (cross-coupling) term for two atoms located at positions \mathbf{r}_i and \mathbf{r}_j , respectively.

Considering all pair-wise couplings in an ensemble of $N \gg 1$ atoms, we find [18, 20]

$$0 = -\frac{i}{2} \sum_{j=1}^N V_{\mathbf{r}_i\mathbf{r}_j} \varphi_{\mathbf{r}_j} - (E - \omega_0) \varphi_{\mathbf{r}_i}, \quad (1)$$

where E denotes the complex eigenenergy of the collec-

* paolo.longo@mpi-hd.mpg.de

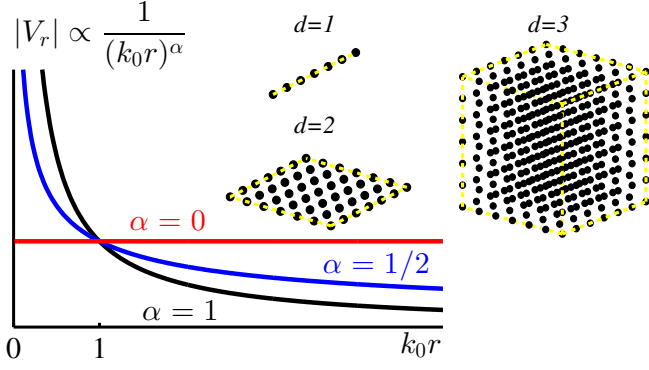


FIG. 1. (color online) Examples for d -dimensional lattices embedded into an electromagnetic reservoir that mediates an inter-atomic coupling $V_r \propto 1/r^\alpha$ [where α characterizes the distance-dependence, see Eq. (6)].

tive single-excitation atomic state $|\Psi\rangle = \sum_{i=1}^N \varphi_{\mathbf{r}_i} \sigma_i^+ |0\rangle$ (σ_i^+ and $|0\rangle$ signify the atomic raising operator for atom i and the vacuum state, respectively). Equation (1) is valid for all dimensions d of the atomic arrangement and for all (physically reasonable) couplings $V_{\mathbf{r}_i \mathbf{r}_j}$. Before we proceed with the study of extended samples, it is worthwhile to demonstrate how Dicke's results emerge here. In the small-volume limit ($a \ll \lambda_0$), the length scale set by the inter-atomic distance a is effectively eliminated, i.e., $V_{\mathbf{r}_i \mathbf{r}_j} \rightarrow V_0$, and all atoms couple to each other with equal strength. The resulting equation $E - \omega_0 = -(i/2)V_0 \sum_{j=1}^N \varphi_{\mathbf{r}_j} / \varphi_{\mathbf{r}_i}$ (which must hold for all \mathbf{r}_i) yields a maximal decay rate for a spatially constant wavefunction with equal relative phase between all atom pairs, representing the maximally symmetric Dicke state. As mentioned in the introduction, this results in a collective decay rate $\Gamma \equiv -2\text{Im}(E) = N\gamma_0 = \chi_{\text{Dicke}}\gamma_0$ and a frequency shift $\Delta \equiv \text{Re}(E) - \omega_0 = \chi_{\text{Dicke}}\delta\omega_0$, with an enhancement factor χ_{Dicke} .

In order to describe an extended sample, we consider ordered atomic arrangements, and focus on chains ($d = 1$), square lattices ($d = 2$), and simple cubic lattices ($d = 3$), see Fig. 1. The smallest inter-atomic distance is given by the lattice constant a . Such ordered arrays are naturally provided by crystalline samples, e.g., solid state targets employed in x-ray quantum optics [6–11]. Other implementations include optical lattices of atoms [22], or atom-cavity networks [23], to name just a few. On the other hand, the assumption of an ordered lattice permits an extensive analytical description.

For a lattice, the plane wave ansatz $\varphi_{\mathbf{r}} = (1/\sqrt{N})e^{i\mathbf{k}\mathbf{r}}$ for Eq. (1) yields the eigenstates' decay rates and frequency shifts

$$\Gamma_{\mathbf{k}} = \gamma_0 + \text{Re}[\mathcal{I}_d(\mathbf{k})], \quad (2)$$

$$\Delta_{\mathbf{k}} = \delta\omega_0 + \frac{1}{2}\text{Im}[\mathcal{I}_d(\mathbf{k})], \quad (3)$$

$$\mathcal{I}_d(\mathbf{k}) = \sum_{\mathbf{r}}' V_r e^{-i\mathbf{k}\mathbf{r}}. \quad (4)$$

Here, $\mathbf{r} = (x_1, \dots, x_d)^T$ denotes a d -dimensional lattice vector with components $x_i = an_i$, $i = 1, \dots, d$, $n_i = -\sqrt[d]{N}/2 + 1, \dots, \sqrt[d]{N}/2$, and $\sqrt[d]{N}$ is even (the sample volume is $\mathcal{V} = Na^d$). Likewise, $\mathbf{k} = (k_1, \dots, k_d)^T$ is the wavevector of the collective atomic excitation. The sum runs over all combinations of $\{n_i\}$ except $n_1 = \dots = n_d = 0$ and the couplings depend on the distance $r = |\mathbf{r}| = a\sqrt{n_1^2 + \dots + n_d^2}$ between atoms. For the remainder, we assume the atomic dipole moments to be uniformly aligned along the x_3 axis (e.g., by applying a weak magnetic field). Thus, for $d = 1, 2$ the distance vector \mathbf{r} (in the x_1 - x_2 plane) is perpendicular to the dipole moments, and for $d = 3$ we have to take into account the polar angle $\theta = \arccos(x_3/r)$. The decay rate (2) can be rewritten in terms of the enhancement factor

$$\chi_{\mathbf{k}} \equiv \frac{\Gamma_{\mathbf{k}}}{\gamma_0} = 1 + \frac{\text{Re}[\mathcal{I}_d(\mathbf{k})]}{\gamma_0}. \quad (5)$$

To calculate the central quantity \mathcal{I}_d , we consider a general type of interatomic couplings

$$\frac{V_r}{\gamma_0} = A_d \sin^2 \theta \frac{e^{i\epsilon k_0 r}}{(k_0 r)^\alpha} \quad (\alpha \geq 0, \epsilon = \pm), \quad (6)$$

where the coefficient α classifies the distance-dependence and A_d is a dimensionless constant (A_d is real for $d = 1, 2$, whereas it is purely imaginary for $d = 3$). Interatomic couplings comprising multiple terms of type (6) can be accounted for by a linear combination (e.g., as realized in the case of three-dimensional free space where the leading order term is $V_r/\gamma_0 = (-3i/2)\sin^2 \theta e^{ik_0 r}/(k_0 r)$ [18, 20, 24]). Equation (6) also includes atoms confined to two spatial dimensions, where $V_r/\gamma_0 \sim H_0^{(1)} \sim e^{ik_0 r}/\sqrt{k_0 r}$ (which is a consequence of the solution to the two-dimensional Helmholtz equation [25] and $H_0^{(1)}$ signifies the zeroth order Hankel function of first kind). As another example, atoms coupled to a one-dimensional waveguide for which (in the absence of damping) $V_r/\gamma_0 \sim e^{ik_0 r}$ [26] can also be accounted for by Eq. (6).

For the remainder, we make use of the assumptions $N \gg 1$ (many atoms) and $k_0 a > 1$ (extended sample). We focus on the system's eigenstates and—to keep the analysis general—do not consider geometric details or questions of how to excite and probe the system. Such aspects vary from experiment to experiment (compare, e.g., atoms in free space to nuclei in a thin-film cavity). Technical details of the calculation can be found in the appendix.

Around $k \equiv |\mathbf{k}| = k_0$, which will turn out to be the relevant wave number region below, we can utilize a continuum formulation [27], rewrite the lattice sums in Eq. (4) into an integral, and perform the angular integration, leading to

$$\frac{\mathcal{I}_d}{\gamma_0} = \frac{2c_d}{(k_0 a)^d} \cdot \left(\frac{k}{k_0}\right)^{\frac{1}{2}(d-1)} \cdot A_d \cdot \mathcal{J}_d(k), \quad (7)$$

d	$\text{Re}[A_d]$	$\text{Im}[A_d]$	b_d	c_d	$j_d(\cdot)$
1	≥ 0	$= 0$	1	1	$\cos(\cdot)$
2	≥ 0	$= 0$	$\frac{1}{\sqrt{\pi}}$	$\sqrt{2\pi}$	$\cos(\cdot)$
3	$= 0$	≤ 0	$\sqrt[3]{\frac{3}{4\pi}}$	$2\pi \cdot \sin^2 \vartheta$	$\sin(\cdot)$

TABLE I. Quantities in Eqs. (7) and (8) as function of the system dimension d . Here, $\vartheta = \arccos(\mathbf{k}\hat{\mathbf{e}}_{x_3}/k)$ denotes the angle between the eigenstate's wavevector \mathbf{k} and the x_3 axis.

$$\mathcal{J}_d(k) = \int_{k_0 a}^{k_0 a b_d \sqrt[4]{N}} d\eta e^{i\eta} j_d(k k_0^{-1} \eta) \eta^\beta, \quad (8)$$

$$\beta \equiv \frac{d-1}{2} - \alpha. \quad (9)$$

The dimension-dependent quantities A_d , b_d , c_d , and j_d are listed in Tab. I. All properties of the system's eigenstates are thus reduced to a detailed understanding of the integral (8). For instance, for $d = 1, 2$, $\text{Re}[\mathcal{J}_d]$ plays the role of the eigenstate's decay rate, whereas $\text{Im}[\mathcal{J}_d]$ describes the frequency shift [for $d = 3$ the roles of $\text{Re}[\mathcal{J}_d]$ and $\text{Im}[\mathcal{J}_d]$ are interchanged, see also Eqs. (2) and (3)].

Results.— The explicit calculation of Eq. (8) reveals that those states whose wavevector's magnitude matches the wavenumber set by the single atom transition, i.e., $k = k_0$, exhibit the maximum possible decay rate which is enhanced by a factor of (cf. Eq. (5))

$$\chi_{\max} \equiv \chi_{k=k_0} = 1 + \frac{|A_d| c_d (b_d)^{\beta+1}}{\beta+1} (k_0 a)^{\beta+1-d} \sqrt[4]{N}^{\beta+1}, \quad (10)$$

if the constraint

$$0 \leq \alpha < \frac{d+1}{2}, \quad (11)$$

i.e., $\beta > -1$, is fulfilled. Equation (11) is a necessary condition for the emergence of superradiance and represents bounds on the allowed power laws of the coupling terms (exponent α in Eq. (6)) as a function of the lattice dimension d . Note that the maximum possible coefficient is realized for $d = 3$ (leading to an upper bound of $\alpha < 2$). For the remainder, we assume that Eq. (11) is fulfilled.

For a given system, the maximum enhancement factor χ_{\max} represents a natural scale on which we base the subsequent discussion. In terms of N , \mathcal{V} , and $\rho = N/\mathcal{V}$, the enhancement factor (10) can be cast into the equivalent forms (note that $\chi_{\max} - 1 \simeq \chi_{\max}$ since $N \gg 1$)

$$\frac{\chi_{\max}}{L(d, \alpha)} = \left(\frac{\lambda_0}{\sqrt[4]{\mathcal{V}}} \right)^{\frac{1}{2}(d-1)+\alpha} \cdot N \quad (N, \mathcal{V}) \quad (12)$$

$$= \left(\frac{\lambda_0}{\sqrt[4]{\mathcal{V}}} \right)^{\frac{1}{2}(d-1)+\alpha} \cdot \mathcal{V} \cdot \rho \quad (\mathcal{V}, \rho)$$

$$= (\lambda_0 \sqrt[4]{\rho})^{\frac{1}{2}(d-1)+\alpha} \cdot \sqrt[4]{N}^{\frac{1}{2}(d+1)-\alpha} \quad (N, \rho),$$

$$L(d, \alpha) \equiv \frac{2(b_d)^{\frac{1}{2}(d+1)-\alpha} c_d}{d+1-2\alpha} \cdot \frac{|A_d|}{(2\pi)^{\frac{1}{2}(d-1)+\alpha}}.$$

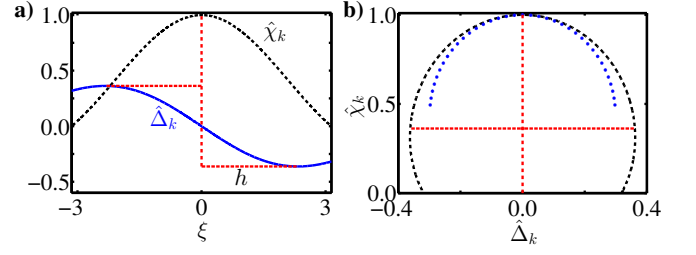


FIG. 2. (Color online) a) Decay rates (black dashed curve) and frequency shifts (blue solid curve) as function of the wavenumber for $\beta = 0$. The figure is valid independent of dimensionality and coupling type, due to the scaling of decay rate $\hat{\chi}_k \equiv (\chi_k - 1)/(\chi_{\max} - 1)$, shift $\hat{\Delta}_k \equiv [(\Delta_k - \delta\omega_0)/\gamma_0]/[\epsilon(\chi_{\max} - 1)]$ and wavenumber $\xi \equiv (k - k_0)ab_d \sqrt[4]{N}$. Note the offset h between the extrema of the frequency shift and the decay rate maximum. b) Decay rates versus frequency shift of the different eigenmodes. The black dashed line denotes the modes shown in a) obtained from the continuum model Eqs. (13) and (14). Blue asterisks show results from a numerical solution of the full eigenproblem (1) for $d = 1$ [29]. Deviations occur for $|\xi| \gtrsim \pi$ where the continuum formulation is not applicable. The region around the maximum superradiant state is well described by the continuum formulation.

Which formulation to choose from Eqs. (12) depends on which quantities can be controlled in an experiment.

For a large but finite system, also states with a wavenumber close to k_0 can exhibit an enhanced decay rate. We illustrate this for the most relevant case $\beta = 0$, which includes the three realizations mentioned in the beginning and which we will also discuss later. For $|k - k_0|a \ll 1$, we find

$$\frac{\Gamma_k}{\gamma_0} = \chi_k \simeq 1 + (\chi_{\max} - 1) \cdot \text{sinc}(\xi), \quad (13)$$

$$\frac{\Delta_k - \delta\omega_0}{\gamma_0} \simeq \epsilon \cdot \frac{\chi_{\max} - 1}{2} \cdot \frac{\cos(\xi) - 1}{\xi}, \quad (14)$$

where $\xi \equiv (k - k_0)ab_d \sqrt[4]{N}$ and $\text{sinc}(\xi) \equiv \sin(\xi)/\xi$. These expressions can be understood as a finite-size correction to the limit of an infinite system [28]. Results are shown in Fig. 2, scaled in such a way that they encompass different dimensions and coupling types. Note that those states which are maximally superradiant at $k = k_0$ do not exhibit a collective frequency shift. Rather, the frequency shift's first two extrema around k_0 occur at wavenumbers $k_{\pm} \equiv k_0 \pm h/(ab_d \sqrt[4]{N})$, where $h \simeq 2.3311$, leading to $(\Delta_{k_{\pm}} - \delta\omega_0)/\gamma_0 \simeq \mp \epsilon \cdot 0.3623 \cdot (\chi_{\max} - 1)$. This finding represents a unique feature as it is independent of the actual realization of the case $\beta = 0$. Furthermore, it provides a signature that can be tested experimentally and is therefore of direct relevance for the characterization of the collective eigenstates in the context of, e.g., x-ray quantum optics in thin-film cavities.

Examples.— We now return to the three examples of possible physical realizations mentioned before. For a chain of qubits coupled to each other via a one-dimensional waveguide [26] ($d = 1$, $\alpha = 0$), the en-

enhancement factor simply becomes $\chi_{\max} = |A_1|N = |A_1|\chi_{\text{Dicke}}$, where $|A_1|$ stands for the (dimensionless) qubit-waveguide coupling strength. Such a system effectively allows for the emergence of small-volume superradiance, even though the inter-atomic distance can be much larger than a wavelength. For an extended sample of atoms in two dimensions, e.g., in the context of x-ray quantum optics, where photons mediating the coupling between ^{57}Fe nuclei in a thin-film cavity essentially propagate in just two spatial dimensions ($d = 2$, $\alpha = 1/2$), the enhancement factor is $\chi_{\max} = (|A_2|/\sqrt{2\pi})\sqrt{\lambda_0^2/\mathcal{V}}\chi_{\text{Dicke}}$ ($|A_2|$ is a coupling constant describing a guided mode of the cavity slab). Also here, superradiance emerges although the atom separation is larger than the wavelength. However, compared to the small-volume case, the enhancement factor is reduced by a factor of $\lambda_0/\sqrt{\mathcal{V}} \ll 1$ (here, \mathcal{V} denotes an area) which takes the extent of the sample into account. Finally, atoms embedded in three-dimensional free space ($d = 3$, leading order $\alpha = 1$ [30], $A_3 = -3i/2$ [18, 20]) give rise to $\chi_{\max} = (3/4\pi)^{4/3}\sin^2\vartheta\sqrt{\lambda_0^3/\mathcal{V}^2}\chi_{\text{Dicke}}$. Here, the superradiant enhancement is reduced by a factor of $(\lambda_0/\sqrt[3]{\mathcal{V}})^2$ relative to the small-volume limit. This result is in line with the findings in the context of a spherical cloud of atoms [14], where the same $1/r$ -integration kernel has been used for determining the decay rate (differences are only due to geometrical prefactors and the averaging over the dipole orientation).

Classification and Scaling.— To be able to identify similarities between different superradiant systems, we further analyze how the enhancement factor (12) depends on experimentally relevant quantities. Suppose that, without loss of generality, we can control the atom number and the volume such that $N \rightarrow f_N N$ and $\mathcal{V} \rightarrow f_V \mathcal{V}$, respectively, where f_N and f_V are arbitrary positive real numbers [the number density then transforms accordingly as $\rho \rightarrow (f_N/f_V)\rho$]. Under this transformation, the enhancement factor changes as

$$\chi_{\max} \rightarrow f_N \sqrt[3]{f_V}^{\frac{1}{2}(1-d-2\alpha)} \chi_{\max}. \quad (15)$$

This behavior allows us to classify and compare superradiant states in systems with different dimensionality

and types of coupling. In fact, Eq. (15) provides a link with which knowledge about the superradiance properties of one system can be transferred to another. For instance, we may say that two extended samples characterized by (d, α) and (d', α') , respectively, are similar if they satisfy the same transformation rule (15), leading to $(\alpha - 1/2)/d = (\alpha' - 1/2)/d'$. As an example, if a one-dimensional system ($d' = 1$) should “imitate” the superradiant state from three-dimensional free space ($d = 3$, $\alpha = 1$), the electromagnetic environment would have to be “engineered” such that $\alpha' = 2/3$. Similarly, if an extended sample should realize small-volume superradiance, transformation (15) must reproduce the transformation of a Dicke system, which is simply $\chi_{\text{Dicke}} = N \rightarrow f_N \cdot \chi_{\text{Dicke}}$. Hence, $\alpha = (1 - d)/2 \geq 0$, which reveals that only extended samples in one dimension ($d = 1$, otherwise we would have $\alpha < 0$) can behave “Dicke-like”. Moreover, as an application, Eqs. (12) and (15) can also be utilized for the design of systems with desired superradiance properties.

Another approach towards classifying systems exhibiting superradiant states is to select the subset of transformations from Eq. (15) which leave the enhancement factor invariant, requiring $f_N f_V^{\frac{1}{2}(1-d-2\alpha)/d} = 1$. In particular, for the case $\beta = 0$, an invariant transformation is given by $f_N = (f_V)^{(d-1)/d}$, where f_V is freely tunable, changing the density as $\rho \rightarrow \rho/\sqrt[3]{f_V}$. For $d = 1$, this means that the atom number remains unchanged ($f_N = 1$) while the system length can in principle become arbitrarily large, leading to an arbitrarily thin medium. Note that a transformation with a constant density, i.e., $f_N = f_V \equiv f$ resulting in $\chi_{\max} \rightarrow \sqrt[3]{f}^{(1+d-2\alpha)/2} \chi_{\max}$, cannot be invariant as this would violate Eq. (11).

Conclusion.— We have studied superradiance in extended samples. Depending on the dimension and the type of coupling, we deduced a criterion for the emergence of superradiance, explained the connection between collective decay rates and frequency shifts, and utilized the scaling behavior of the enhancement factor for classifying and comparing superradiance in different systems. Our results provide a “bridge” between the various theoretical and experimental approaches towards superradiance in extended media, and can be used to design the properties of superradiant systems.

-
- [1] R. H. Dicke, Phys. Rev. **93**, 99 (1954).
 - [2] M. Gross and S. Haroche, Phys. Rev. **93**, 301 (1982).
 - [3] F. L. Kien, S. D. Gupta, K. P. Nayak, and K. Hakuta, Phys. Rev. A **72**, 063815 (2005).
 - [4] J. Keaveney, A. Sargsyan, U. Krohn, I. G. Hughes, D. Sarkisyan, and C. S. Adams, Phys. Rev. Lett. **108**, 173601 (2012).
 - [5] J. Pellegrino, R. Bourgain, S. Jennewein, Y. R. P. Sordais, A. Browaeys, S. D. Jenkins, J. Ruostekoski, arXiv:1402.4167 (2014).
 - [6] R. Röhlsberger, K. Schlage, B. Sahoo, S. Couet, and

- R. Rüffer, Science **328**, 1248 (2010).
- [7] R. Röhlsberger, H.-C. Wille, K. Schlage, and B. Sahoo, Nature **482**, 199 (2012).
- [8] K. P. Heeg, H.-C. Wille, K. Schlage, T. Guryeva, D. Schumacher, I. Uschmann, K. S. Schulze, B. Marx, T. Kämpfer, G. G. Paulus, R. Röhlsberger, and J. Evers, Phys. Rev. Lett. **111**, 073601 (2013).
- [9] K. P. Heeg, J. Haber, D. Schumacher, L. Bocklage, H.-C. Wille, K. S. Schulze, R. Loetzsch, I. Uschmann, G. G. Paulus, R. Rüffer, R. Röhlsberger, and J. Evers, arXiv:1409.0365 [quant-ph].

- [10] K. P. Heeg, C. Ott, D. Schumacher, H.-C. Wille, R. Röhlsberger, T. Pfeifer, and J. Evers, arXiv:1411.1545 [quant-ph].
- [11] K. P. Heeg and J. Evers, Phys. Rev. A **88**, 043828 (2013).
- [12] R. Friedberg, S. R. Hartmann, and J. T. Manassah, Phys. Rep. **7**, 101 (1973).
- [13] R. Friedberg and J. T. Manassah, Phys. Lett. A **372**, 6833 (2008).
- [14] M. O. Scully and A. A. Svidzinsky, Phys. Lett. A **373**, 1283 (2009).
- [15] A. A. Svidzinsky and M. O. Scully, Opt. Commun. **283**, 753 (2010).
- [16] R. Friedberg and J. T. Manassah, Phys. Lett. A **373**, 3423 (2009).
- [17] Z. Ficek and S. Swain, *Quantum Interference and Coherence*, Springer, New York (2005).
- [18] Y. Li, J. Evers, H. Zheng, and S.-Y. Zhu, Phys. Rev. A **85**, 053830 (2012).
- [19] P. Longo and J. Evers, Phys. Rev. Lett. **112**, 193601 (2014).
- [20] P. Longo and J. Evers, Phys. Rev. A **90**, 063834 (2014).
- [21] G. S. Agarwal, *Quantum Statistical Theories of Spontaneous Emission and their Relation to Other Approaches*, Springer, Berlin (1974).
- [22] D. Jacksch and P. Zoller, Ann. Phys. **315**, 52 (2005).
- [23] A. Kay and D.G. Angelakis, Europhys. Lett. **84**, 20001 (2008).
- [24] L. Bellando, A. Gero, E. Akkermans, and R. Kaiser, Phys. Rev. A **90**, 063822 (2014).
- [25] R. T. Couto, Revista Brasileira de Ensino de Física **35**, 1304 (2013).
- [26] A. Gonzalez-Tudela, D. Martin-Cano, E. Moreno, L. Martin-Moreno, C. Tejedor, and F. J. Garcia-Vidal, Phys. Rev. Lett. **106**, 020501 (2011).
- [27] The factor $\exp(\pm ik_0 r)$ from Eq. (6) in the eigenproblem (1) can be understood as a translation in wavenumber space reciprocal to the radial direction. In the shifted frame, a long-wavelength limit of the collective atomic excitation (which can be accounted for by a continuum description) corresponds to $k \rightarrow k_0$. This continuum formulation is applicable in the range $|k - k_0| \lesssim \pi/ab_d \sqrt[4]{N}$.
- [28] In Eq. (6), we have not included exponential damping of the form $\exp(-k_0 r/\ell)$, where ℓ denotes a dimensionless absorption length that, for instance, empirically accounts for material imperfections. This damping factor in the integral (8) would lead to a broadening and modification of the $k = k_0$ -criterion for maximal superradiance. This analysis is beyond the scope of this paper.
- [29] We have solved Eq. (1) for $d = 1$ ($\alpha = 0$) by means of exact diagonalization on a finite lattice for various k_0 ($k_0 a$ in a range from $-\pi$ to π around a multiple of 2π ; the problem is 2π periodic with respect to $k_0 a$).
- [30] Note that the next leading order term realizes $\alpha = 2$, which violates Eq. (11) and therefore does not support superradiant states.

Appendix A: $\mathcal{I}_d(\mathbf{k})$

The quantity

$$\mathcal{I}_d(\mathbf{k}) = \sum_{n_1}' \dots \sum_{n_d}' V_a \sqrt{n_1^2 + \dots + n_d^2} e^{-ik_1 a n_1} \dots e^{-ik_d a n_d}, \quad (\text{A1})$$

where the sums run over all combinations of $\{n_i\}$ except $n_1 = \dots = n_d = 0$, can be rewritten into an integral

$$\mathcal{I}_d(\mathbf{k}) \rightarrow \int \frac{d^d x}{a^d} V(r, \theta) \prod_{j=1}^d e^{-k_j x_j}. \quad (\text{A2})$$

For $d = 1, 2$, $V(r, \theta) = f_r$, whereas for $d = 3$, $V(r, \theta) = \sin^2 \theta f_r$ ($f_r \equiv A_d \exp(i k_0 r)/(k_0 r)^\alpha$). Here, $d^d x$ signifies the d dimensional infinitesimal volume element and the integration is over all space except for a region with radius a around the origin ($d^1 x = dx$, $d^2 x = r dr d\varphi$, $d^3 x = r^2 \sin \theta dr d\varphi d\theta$).

Explicitly, for $d = 1$,

$$\begin{aligned} \mathcal{I}_1 &= \int_{-\frac{Na}{2}}^{\frac{Na}{2}} \frac{dx}{a} \Theta(|x| - a) f_{|x|} e^{-ikx} \\ &= \int_a^{\frac{Na}{2}} \frac{dx}{a} f_{|x|} 2 \cos(kx) \\ &= 2 \int_a^{\frac{Na}{2}} \frac{dr}{a} f_r \cos(kr), \end{aligned} \quad (\text{A3})$$

where $k = |\mathbf{k}|$ and $\Theta(\cdot)$ signifies the Heaviside step function. For $d = 2$,

$$\begin{aligned} \mathcal{I}_2 &= \int_a^{N'_2 a} \int_0^{2\pi} \frac{r dr d\varphi}{a^2} f_r e^{-ik_1 r \cos \varphi} e^{-ik_2 r \sin \varphi} \\ &= \frac{2\pi}{a^2} \int_a^{N'_2 a} dr r f_r J_0(kr), \end{aligned} \quad (\text{A4})$$

where N'_2 is chosen such that the integration area covers N atoms, i.e., $\pi(N'_2)^2 = N$. For $d = 3$,

$$\begin{aligned} \mathcal{I}_3 &= \int_a^{N'_3 a} \frac{r^2 dr}{a^3} \int_0^\pi d\theta \sin \theta \int_0^{2\pi} d\varphi \underbrace{V(r, \theta)}_{=\sin^2 \theta f_r} \\ &\quad \times e^{-ik_1 r \sin \theta \cos \varphi} e^{-ik_2 r \sin \theta \sin \varphi} e^{-ik_3 r \cos \theta} \\ &= 2\pi \int_a^{N'_3 a} \frac{r^2 dr}{a^3} f_r \int_0^\pi d\theta \sin^3 \theta e^{-ik_3 r \cos \theta} \\ &\quad \times J_0 \left(\sin \theta \sqrt{k_1^2 + k_2^2} r \right), \end{aligned} \quad (\text{A5})$$

where $(4\pi/3)(N'_3)^3 = N$, $J_0(\cdot)$ signifies the zeroth-order Bessel function of first kind, and $\text{sinc}(x) = \sin(x)/x$. The integration over θ can be done as follows. Upon defining $I_m \equiv \int_0^\pi d\theta \sin^m \theta \exp(-ik_\perp r \cos \theta) J_0(k_\parallel r \sin \theta)$, $k_\perp \equiv k_3$, and $k_\parallel \equiv \sqrt{k_1^2 + k_2^2}$, we have the relation

$$\begin{aligned} I_3 &= I_1 - \int_0^\pi d\theta \cos^2 \theta \sin \theta e^{-ik_\perp r \cos \theta} J_0(k_\parallel r \sin \theta) \\ &= \left(1 + \frac{1}{r^2} \frac{\partial^2}{\partial k_\perp^2} \right) I_1. \end{aligned} \quad (\text{A6})$$

To simplify the integration needed for I_1 , we can choose a coordinate system in which either $k_\perp = 0$ or $k_\parallel = 0$ (it can be shown that I_1 does not depend on the orientation of \mathbf{k}), yielding

$$I_1 = 2 \operatorname{sinc} \left(\sqrt{k_\perp^2 + k_\parallel^2} r \right). \quad (\text{A7})$$

Finally, $I_3 = \sin^2 \vartheta \cdot 2 \operatorname{sinc}(kr) + \mathcal{O}[(kr)^{-2}]$ and therefore

$$\mathcal{I}_3 = \frac{4\pi}{a^3} \sin^2 \vartheta \int_a^{N'_3 a} dr r^2 f_r \operatorname{sinc}(kr), \quad (\text{A8})$$

where ϑ denotes the angle between the eigenstate's wavevector \mathbf{k} and the z axis. Here, we have only taken into account the asymptotic leading order term (with respect to kr). Other terms can be accounted for by means of different coefficients α (see main text). Introducing the abbreviations used in the paper and performing a variable substitution, we finally arrive at the integrals $\mathcal{J}_d(k)$ (Eq. (8) in the paper).

Appendix B: $\mathcal{J}_d(k)$

We now proceed with the radial integration

$$\mathcal{J}_d(k) = \int_{k_0 a}^{k_0 a b_d \sqrt[4]{N}} d\eta e^{\pm i\eta} j_d(k k_0^{-1} \eta) \eta^\beta. \quad (\text{B1})$$

Note that for $d = 2$ the integration kernel is actually given by $J_0(k k_0^{-1} \eta)$. However, already at the lower integration limit, we can use the asymptotic form $J(ka) \approx \sqrt{2/\pi} \cos(ka - \pi/4)/\sqrt{ka}$ since in an extended sample $k_0 a > 1$ and only the wavenumbers k around k_0 are relevant. Furthermore, by an additional substitution of the integration variable, we shift the $\pi/4$ shift to the argument to the exponential (which we can account for by means of appropriate prefactors), $\eta + \pi/4 \approx \eta$, and the integration limits can also approximately remain unchanged.

The possible combinations in the integrand we need to consider are

$$J_{cc} \equiv \int_{k_0 a}^{k_0 a b_d \sqrt[4]{N}} d\eta \cos(\eta) \cos(k k_0^{-1} \eta) \eta^\beta, \quad (\text{B2})$$

$$J_{sc} \equiv \int_{k_0 a}^{k_0 a b_d \sqrt[4]{N}} d\eta \sin(\eta) \cos(k k_0^{-1} \eta) \eta^\beta, \quad (\text{B3})$$

$$J_{cs} \equiv \int_{k_0 a}^{k_0 a b_d \sqrt[4]{N}} d\eta \cos(\eta) \sin(k k_0^{-1} \eta) \eta^\beta, \quad (\text{B4})$$

$$J_{ss} \equiv \int_{k_0 a}^{k_0 a b_d \sqrt[4]{N}} d\eta \sin(\eta) \sin(k k_0^{-1} \eta) \eta^\beta. \quad (\text{B5})$$

1. J_{cc}

Utilizing a computer algebra system, we find that

$$J_{cc} = \frac{i^{\beta+1}}{4} \cdot \left[\left(\frac{r_-}{k_0} \right)^{-1-\beta} (\operatorname{sgn}(r_-))^{-2\beta} \right. \\ \times \left(\Gamma(1+\beta, -ir_- a) - \Gamma(1+\beta, -ir_- a N'_d) - (-1)^\beta \Gamma(1+\beta, ir_- a) + (-1)^\beta \Gamma(1+\beta, ir_- a N'_d) \right) \\ \left. + \left(\frac{r_+}{k_0} \right)^{-1-\beta} \times \left(\Gamma(1+\beta, -ir_+ a) - \Gamma(1+\beta, -ir_+ a N'_d) - (-1)^\beta \Gamma(1+\beta, ir_+ a) + (-1)^\beta \Gamma(1+\beta, ir_+ a N'_d) \right) \right], \quad (\text{B6})$$

where $r_\pm \equiv k \pm k_0$ and $\Gamma(a, z) \equiv \int_z^\infty dt t^{a-1} e^{-t}$ signifies the incomplete Gamma function. The asymptotic form for $N'_d \gg 1$ and $r_- \neq 0$ reads

$$J_{cc}(k \neq k_0) \simeq \frac{i^{\beta+1}}{4} \cdot \left[\left(\frac{r_-}{k_0} \right)^{-1-\beta} (\operatorname{sgn}(r_-))^{-2\beta} \right. \\ \times \left(\Gamma(1+\beta, -ir_- a) - (-1)^\beta \Gamma(1+\beta, ir_- a) - 2i(-1)^\beta (ir_- a N'_d)^\beta \sin(r_- a N'_d) \right) \\ \left. + \left(\frac{r_+}{k_0} \right)^{-1-\beta} \times \left(\Gamma(1+\beta, -ir_+ a) - (-1)^\beta \Gamma(1+\beta, ir_+ a) - 2i(-1)^\beta (ir_+ a N'_d)^\beta \sin(r_+ a N'_d) \right) \right]. \quad (\text{B7})$$

The dominant terms for $N'_d \gg 1$ in this expression are $\propto (N'_d)^\beta$ if $\beta > 0$.

For $k \rightarrow k_0$ ($N'_d = b_d \sqrt[4]{N} \gg 1$), we arrive at

$$J_{cc}(k \rightarrow k_0) \simeq \frac{1}{2(1+\beta)} (k_0 a)^{\beta+1} (N'_d)^{\beta+1} \quad (\text{B8})$$

$$= \frac{(b_d)^{\beta+1}}{2(1+\beta)} (k_0 a)^{\beta+1} N^{\frac{\beta+1}{4}}. \quad (\text{B9})$$

Here, the dominant terms for $N'_d \gg 1$ are $\propto (N'_d)^{\beta+1}$ if $\beta > -1$.

For the case $\beta = 0$, the explicit expression for the

integral reads

$$J_{cc} \stackrel{\beta=0}{=} \frac{k_0 a}{2} \left[N'_d (\text{sinc}(r_- a N'_d) + \text{sinc}(r_+ a N'_d)) - \text{sinc}(r_+ a) - \text{sinc}(r_- a) \right] \quad (\text{B10})$$

$$\stackrel{|r_-|a \ll 1, N'_d \gg 1}{\simeq} \frac{k_0 a}{2} N'_d \text{sinc}(r_- a N'_d)$$

$$\stackrel{k \rightarrow k_0}{\rightarrow} \frac{k_0 a}{2} N'_d = \frac{k_0 a}{2} b_d N^{\frac{1}{d}}.$$

In the second step, we focus on wavenumbers k around k_0 (i. e., small $|r_-|a$).

2. J_{sc}

Similarly,

$$J_{sc} = \frac{i^{\beta+2}}{4} \cdot \left[\left(\frac{r_-}{k_0} \right)^{-1-\beta} (\text{sgn}(r_-))^{-2\beta} \right. \quad (\text{B11})$$

$$\times \left(-\Gamma(1+\beta, -ir_- a) + \Gamma(1+\beta, -ir_- a N'_d) - (-1)^\beta \Gamma(1+\beta, ir_- a) + (-1)^\beta \Gamma(1+\beta, ir_- a N'_d) \right)$$

$$+ \left(\frac{r_+}{k_0} \right)^{-1-\beta} \left(\Gamma(1+\beta, -ir_+ a) - \Gamma(1+\beta, -ir_+ a N'_d) + (-1)^\beta \Gamma(1+\beta, ir_+ a) - (-1)^\beta \Gamma(1+\beta, ir_+ a N'_d) \right) \Big].$$

The asymptotic form for $N'_d \gg 1$ but $r_- \neq 0$ reads

$$J_{sc}(k \neq k_0) \simeq \frac{i^{\beta+2}}{4} \cdot \left[\left(\frac{r_-}{k_0} \right)^{-1-\beta} (\text{sgn}(r_-))^{-2\beta} \right. \quad (\text{B12})$$

$$\times \left(-\Gamma(1+\beta, -ir_- a) - (-1)^\beta \Gamma(1+\beta, ir_- a) + 2(-1)^\beta (ir_- a N'_d)^\beta \cos(r_- a N'_d) \right)$$

$$+ \left(\frac{r_+}{k_0} \right)^{-1-\beta} \left(\Gamma(1+\beta, -ir_+ a) - (-1)^\beta \Gamma(1+\beta, ir_+ a) - 2(-1)^\beta (ir_+ a N'_d)^\beta \cos(r_+ a N'_d) \right) \Big].$$

In contrast to the integral J_{cc} , the limit $k \rightarrow k_0$ does not yield a scaling $\propto (N'_d)^{\beta+1}$. The case $\beta = 0$ reads

$$J_{sc} \stackrel{\beta=0}{=} \frac{k_0 a}{2} \left[\frac{\cos(r_- a N'_d)}{r_- a} - \frac{\cos(r_+ a N'_d)}{r_+ a} - \frac{\cos(r_- a)}{r_- a} + \frac{\cos(r_+ a)}{r_+ a} \right] \quad (\text{B13})$$

$$\stackrel{|r_-|a \ll 1, N'_d \gg 1}{\simeq} \frac{k_0 a}{2} \cdot \frac{\cos(r_- a N'_d) - 1}{r_- a}.$$

3. J_{cs}

We can rewrite

$$J_{cs} = \int_{k_0 a}^{k_0 a b_d \sqrt[d]{N}} d\eta \cos(\eta) \sin(k k_0^{-1} \eta) \eta^\beta \quad (\text{B14})$$

$$= \left(\frac{k_0}{k} \right)^{\beta+1} \int_{ka}^{kab_d \sqrt[d]{N}} d\eta \sin(\eta) \cos(k_0 k^{-1} \eta) \eta^\beta.$$

This is in essence just the integral J_{sc} with k and k_0 interchanged. In particular, for $\beta = 0$, $J_{cs} = -J_{sc}$.

4. J_{ss}

For $k \rightarrow k_0$, we can write

$$J_{ss}(k \rightarrow k_0) = \int_{k_0 a}^{k_0 a b_d \sqrt[d]{N}} d\eta (1 - \cos^2 \eta) \eta^{\beta+1} \quad (\text{B15})$$

$$= \underbrace{(k_0 a b_d \sqrt[d]{N})^{\beta+1} - (k_0 a)^{\beta+1}}_{2J_{cc}(k \rightarrow k_0)} - J_{cc}(k \rightarrow k_0)$$

$$\stackrel{N \gg 1}{\simeq} J_{cc}(k \rightarrow k_0).$$

For $\beta = 0$, the explicit expression reads

$$J_{ss} \stackrel{\beta=0}{=} \frac{k_0 a}{2} \left[N'_d (\text{sinc}(r_- a N'_d) - \text{sinc}(r_+ a N'_d)) + \text{sinc}(r_+ a) - \text{sinc}(r_- a) \right] \quad (\text{B16})$$

$$\stackrel{|r_-|a \ll 1, N'_d \gg 1}{\simeq} \frac{k_0 a}{2} N'_d \text{sinc}(r_- a N'_d).$$